

Nanoscale metal/self-assembled monolayer/metal heterostructures

C. Zhou,^{a)} M. R. Deshpande, and M. A. Reed^{b)}

Center for Microelectronic Materials and Structures, Yale University, New Haven, Connecticut 06520-8284

L. Jones II and J. M. Tour

Department of Chemistry and Biochemistry, University of South Carolina, Columbia, South Carolina 29208

(Received 17 April 1997; accepted for publication 30 May 1997)

We present the investigation of novel metal/organic monolayer/metal heterostructure diodes. Our technique provides well-defined, stable, and reproducible metallic contacts to a self-assembled monolayer of 4-thioacetyl biphenyl with nanoscale area. Electronic transport measurements show a prominent rectifying behavior arising from the asymmetry of the molecular heterostructure. Variable-temperature measurements reveal that thermal emission of electrons over a barrier of 0.22 eV dominates for electron injection from Ti into the organic layer while the transport for electron injection from Au into the organic layer satisfies the formula for hopping conduction. © 1997 American Institute of Physics. [S0003-6951(97)q0131-9]

Research on molecular electronics has provided a large number of molecular wire candidates.¹ With their linear chain structure and the dominant electron delocalization along the chain, these molecular wires are expected to exhibit novel electronic and optical properties which could find applications in future very large scale integrated (VLSI) circuits.¹⁻⁸ In spite of the utmost technological importance, the conductivity and transport mechanisms of these molecular wires are not well understood. The reasons lie in the difficulty of preparing well-defined, stable, and reproducible metallic contacts to the two ends of the molecular wires. Scanning tunneling microscope (STM) has been used to resolve images of single molecules;³ however, these experiments could not give the absolute value of the conductivity due to the involvement of a tunneling gap between the STM tip and the molecule. Reifenberger *et al.* have developed a method to deduce the zero-bias conductivity of an ensemble of molecular wires,^{4,5} nevertheless, the bias range applied across the molecules is small and hence no information concerning current-voltage spectroscopy has been derived. Direct contacting to organic thin films has been executed;⁷ however, multilayers of the molecular wires and micron scale area of the devices containing a large number of molecules have been used, which complicates the analysis of the transport mechanism of single molecules. Direct contacting to and electrical measurements of a single monolayer of a small number of molecules has not yet been demonstrated.

Here we introduce a novel fabrication technique to directly measure the conduction through a small number of organic molecules. These devices consist of a self-assembled monolayer (SAM) of conjugated molecular wires sandwiched between top and bottom metallic contacts. This technique guarantees good control over the device area and intrinsic contact stability. Two essential features are included in the process, the first of which is the employment of nanoscale device area. The area is made to be smaller than the domain size of the SAM and thus the adsorbed organic layer is highly ordered and mostly defect free. The second feature

is that during the deposition of the top contact, several measures are taken to ensure that the deposited metal atoms accumulate at the SAM surface and do not penetrate into the organic layer. These methods also provide minimized damage to the SAM during the deposition.

A schematic diagram of the device is shown in Fig. 1. E-beam lithography and following plasma etching are used to open a pore in the suspended (LPCVD) SiN membrane.⁹ The pore takes a bowl shape with the opening at the upper

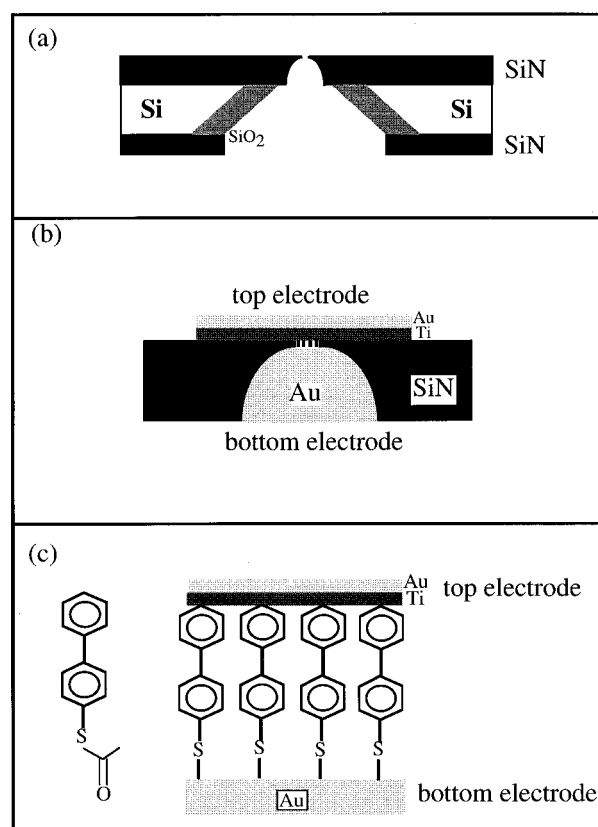


FIG. 1. Fabrication of the heterostructure. (a) Cross section of a silicon wafer showing the bowl-shaped pore etched in suspended SiN membrane with a diameter about 300 Å. (b) Au-Ti top electrode/self-assembled monolayer/Au bottom electrode sandwich structure in the nanopore. (c) 4-thioacetyl biphenyl and detail diagram of the sandwich heterostructure.

^{a)}Electronic mail: zhou@optik.eng.yale.edu

^{b)}Electronic mail: reed@surf.eng.yale.edu

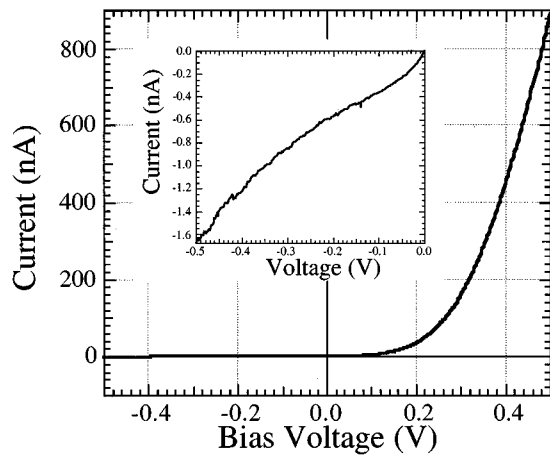


FIG. 2. I - V characteristics at room temperature. Magnified view of the negative bias part in the inset.

edge having a diameter of ~ 30 nm, as shown in Fig. 1(a). Gold is evaporated from the bottom side to fill the pore. The typical crystallite size for gold is about 50 nm and thus the upper surface of gold in the nanopore is probably a single crystallite. The samples are then immediately immersed into 0.3 millimolar solution of the organic molecules for three days under argon atmosphere. The molecules we use are 4-thioacetylphenyl, as shown in Fig. 1(c) with a length about 12 Å. It has been demonstrated that under such conditions the functionalized organic molecules would self-assemble onto the gold surface and form a highly ordered monolayer.¹ After the formation of the SAM, the samples are taken out of the solution and loaded into a high vacuum chamber of 10^{-8} Torr to deposit the top electrode. First, 10 Å Ti is deposited onto the upper surface of the SAM. This amount of Ti would bond onto the SAM surface and form a continuous film.¹⁰ The samples are then maintained at low temperature while 30 Å Ti and 800 Å Au is deposited onto the upper side of the samples, which is thick enough to make the top electrodes continuous and well conducting. This low-temperature deposition helps to minimize the thermal damage to the SAM. A very low deposition rate (~ 0.3 Å/s) is also used for the same reason. A detailed schematic of the sandwiched heterostructure is shown in Figs. 1(b) and 1(c). The samples are then allowed to slowly warm up to room temperature (~ 24 h). This technique gives us a yield of about 80% working devices. These devices are stable at room temperature and vary only slightly after thermal cycling to ~ 50 K.

Two terminal current (I)-voltage (V) characteristics are measured in the temperature range from room temperature down to 57 K. Figure 2 shows the I - V curves of the device measured at room temperature. Positive bias corresponds to electrons emitted from the Au/Ti top electrode and collected by the bottom Au electrode. I - V characteristics under negative bias are shown in the inset of Fig. 2. Prominent rectifying behavior is observed: the current at 1 V bias is about 500 times higher than the current at -1 V bias. While the I - V curve at negative bias is rather linear, the I - V curve at positive bias displays exponential behavior. For different devices, the current magnitude varies slightly due to variation

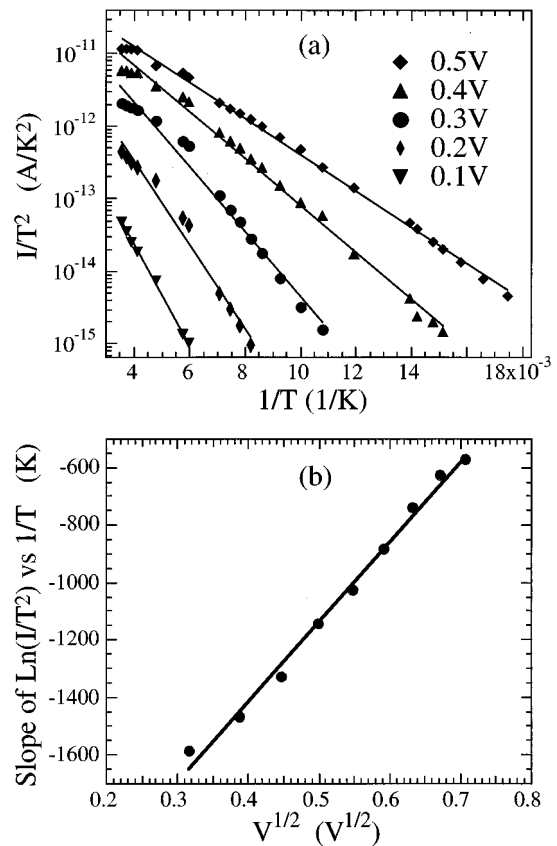


FIG. 3. (a) Plots of $\ln(I/T^2)$ vs $1/T$ for a series of positive bias voltages. The straight lines are least-square fits to the data points for each bias. (b) Plot of the slope of the fitted lines in (a) vs $V^{1/2}$. The slope and intercept of the fitted straight line give the value of a and $q\Phi$.

in device area, but the rectifying behavior is always observed.

The current is observed to decrease monotonically with temperature under both positive and negative biases. At 1 V positive bias the current experiences about four orders of magnitude decrease as temperature decreases from room temperature to 57 K, suggesting a thermally activated transport mechanism. For thermally activated electron injection from the metal into the SAM, the image force potential causes a lowering of the barrier height and the formula accounting for both thermal activation and image force potential is given by:^{11,12}

$$I = AT^2 e^{a\sqrt{V} - q\Phi/kT}, \quad \text{where } a = \frac{q}{2} \sqrt{\frac{q}{4\pi\epsilon_i\epsilon_0 d}}, \quad (1)$$

where A is the effective Richardson constant multiplied by the current injection area, q the electron charge, Φ the thermal emission barrier height, V the bias, k Boltzmann's constant, T the temperature, ϵ_i the relative dielectric constant of the SAM, ϵ_0 the vacuum dielectric constant, and d the thickness of the molecular dielectric film. Figure 3(a) displays the plots of $\ln(I/T^2)$ vs $1/T$ for different biases, where the marks represent data points and the lines are least-square fits for each bias. The plots clearly demonstrate that $\ln(I/T^2)$ is linear with $1/T$ and the slopes of the lines is a function of the bias voltage. The standard thermal emission theory predicts:

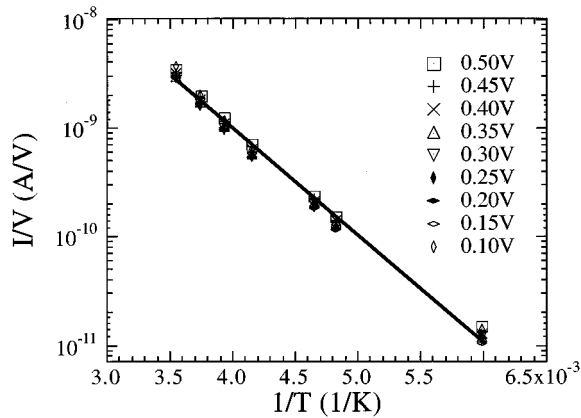


FIG. 4. Plot of I/V vs $1/T$ for different negative biases. The data points collapse onto one line, indicating hopping conduction.

$$\text{slope} = \frac{a\sqrt{V} - q\Phi}{k} \quad \text{and} \quad \text{intercept} = \ln A. \quad (2)$$

One can plot the slope of each line in Fig. 3(a) vs $V^{1/2}$ and determine the constants a and $q\Phi$, as shown in Fig. 3(b). The data points are found to lie on a straight line and the least-square fitting yields a value of 0.22 eV for $q\Phi$ and 0.239 eV $^{1/2}$ for a . Given the film thickness of 10 Å as measured from the ellipsometry data, from formula (1), we can further determine the dielectric constant of the SAM to be 6.3. From the intercepts of the lines in Fig. 3(a), one can obtain a value of 7.5×10^{-11} A for A .

The negative bias corresponds to electrons injected from the Au bottom electrode into the conjugated molecules through the thiolates. The current also decreases with temperature; however, detailed analysis reveals that the data fit the hopping conduction mechanism: $I \propto V e^{-c/kT}$, which corresponds to electrons hopping from one site to the neighboring ones.^{11,13} For different biases, plots of $\ln(I/V)$ vs $1/T$ fall on one line, as shown in Fig. 4. The least-square fitting yields a hopping barrier of 0.19 eV. At present it is unclear whether the hopping is related to defects in the SAM, hopping along the molecular wire or hopping between neighboring molecular wires. Gold is known to have a higher work function than Ti; despite the lack of knowledge about the interface states and the role of sulfur atoms, these results suggest that the barrier for electrons injected from the bottom

gold electrode is higher than the barrier for electrons injected from the top Ti electrode. As a result, no prominent thermal emission is observed under negative bias and the current is carried by electrons hopping through the molecular layer instead of electrons thermally activated over the Au/SAM barrier.

In conclusion, we have demonstrated a new fabrication technique to study the transport mechanism of organic molecular wires. Nanoscale device area and special metal deposition techniques are employed to provide intrinsically stable and highly reproducible metallic contacts to the self-assembled monolayer of a small number of conjugated molecular wires with a length of 12 Å. Due to the asymmetry in the heterostructure, prominent rectifying behavior is observed in the $I-V$ characteristics. Under positive bias, electrons are thermally activated and injected from Ti into the SAM with a thermal emission barrier of 0.22 eV while hopping conduction is found to dominate under negative bias. This method can be easily adapted to other molecular wire systems for determination of transport mechanisms and band alignment.

- ¹J. M. Tour, L. Jones II, D. L. Pearson, J. J. S. Lamba, T. P. Burgin, G. M. Whitesides, D. L. Allara, A. N. Parikh, and S. V. Atre, *J. Am. Chem. Soc.* **117**, 9529 (1995).
- ²M. P. Samanta, W. Tian, S. Datta, J. I. Henderson, and C. P. Kubiak, *Phys. Rev. B* **53**, R7626 (1996).
- ³L. A. Bumm, J. J. Arnold, M. T. Cygan, T. D. Dunbar, T. P. Burgin, L. Jones II, D. L. Allara, J. M. Tour, and P. S. Weiss, *Science* **271**, 1705 (1996).
- ⁴R. P. Andres, T. Bein, M. Dorogi, S. Feng, J. I. Henderson, C. P. Kubiak, W. Mahoney, R. G. Osifchin, and R. Reifenberger, *Science* **272**, 1323 (1996).
- ⁵M. Dorogi, J. Gomez, R. Osifchin, R. P. Andres, and R. Reifenberger, *Phys. Rev. B* **52**, 9071 (1995).
- ⁶A. Stabel, P. Herwig, K. Müllen, and J. P. Rabe, *Angew. Chem. Int. Ed. Engl.* **34**, 1609 (1995).
- ⁷C. M. Fischer, M. Burghard, S. Roth, and K. v. Klitzing, *Appl. Phys. Lett.* **66**, 3331 (1995).
- ⁸M. A. Reed, U.S. Patent No. 5,475,341 (December 12, 1995).
- ⁹K. S. Ralls, R. A. Buhrman, and R. C. Tiberio, *Appl. Phys. Lett.* **55**, 2459 (1989).
- ¹⁰K. Konstadinidis, P. Zhang, R. L. Opila, and D. L. Allara, *Surf. Sci.* **338**, 300 (1995).
- ¹¹S. M. Sze, *Physics of Semiconductor Devices*, 2nd ed. (Wiley, New York, 1981), p. 403.
- ¹²D. R. Lamb, *Electrical Conduction Mechanisms in Thin Insulating Films* (Methuen, London, 1967), p. 47.
- ¹³K. Okada and K. Taniguchi, *Appl. Phys. Lett.* **70**, 351 (1997).